Preeruptive inflation and surface interferometric coherence characteristics revealed by satellite radar interferometry at Makushin Volcano, Alaska: 1993–2000

Zhong Lu,[1] John A. Power,[2] Vicki S. McConnell,[3] Charles Wicks Jr.,[4] and Daniel Dzurisin[5]

Received 17 August 2001; revised 25 March 2002; accepted 30 March 2002; published 1 November 2002.

[1] Pilot reports in January 1995 and geologic field observations from the summer of 1996 indicate that a relatively small explosive eruption of Makushin, one of the more frequently active volcanoes in the Aleutian arc of Alaska, occurred on 30 January 1995. Several independent radar interferograms that each span the time period from October 1993 to September 1995 show evidence of ~7 cm of uplift centered on the volcano's east flank, which we interpret as preeruptive inflation of a ~7-km-deep magma source ($\Delta V = 0.022$ km^3). Subsequent interferograms for 1995–2000, a period that included no reported eruptive activity, show no evidence of additional ground deformation. Interferometric coherence at C band is found to persist for 3 years or more on lava flow and other rocky surfaces covered with short grass and sparsely distributed tall grass and for at least 1 year on most pyroclastic deposits. On lava flow and rocky surfaces with dense tall grass and on alluvium, coherence lasts for a few months. Snow and ice surfaces lose coherence within a few days. This extended timeframe of coherence over a variety of surface materials makes C band radar interferometry an effective tool for studying volcano deformation in Alaska and other similar high-latitude regions. *INDEX TERMS:* 8494 Volcanology: Instruments and techniques; 6924 Radio Science: Interferometry; 8419 Volcanology: Eruption monitoring (7280); *KEYWORDS:* SAR, InSAR, interferometry, Makushin, deformation, coherence

Citation: Lu, Z., J. A. Power, V. S. McConnell, C. Wicks Jr., and D. Dzurisin, Preeruptive inflation and surface interferometric coherence characteristics revealed by satellite radar interferometry at Makushin Volcano, Alaska: 1993–2000, *J. Geophys. Res.*, *107*(B11), 2266, doi:10.1029/2001JB000970, 2002.

1. Introduction

[2] At least 29 and possibly as many as 41 volcanic centers in the 2500-km-long Aleutian arc have erupted during historical time, producing an average of about two eruptions per year during the latter half of the twentieth century [*Miller et al.*, 1998]. Owing to the remote setting and persistent cloud cover, some Aleutian eruptions likely go unreported, especially those that are small or brief. For the same reasons, the magnitudes of some short-duration eruptions might be underestimated. Consequently, remote sensing plays an important role in monitoring and studying Aleutian volcanoes [*Dean et al.*, 1998]. Satellite interferometric synthetic aperture radar (InSAR) is a remote sensing technique that has been used successfully to study many active volcanoes, including several in the Aleutian arc, during the past few years [e.g., *Massonnet and Feigl*, 1998; *Zebker et al.*, 2000]. Phase information in two SAR images can be processed by applying an interference technique to map ground deformation with cm-scale precision over length scales of a few kilometers to hundreds of kilometers [e.g., *Massonnet and Feigl*, 1998; *Rosen et al.*, 2000].

[3] We describe in this paper the use of InSAR to systematically search for ground deformation near Makushin Volcano in the central Aleutian arc (Figure 1a), using available ERS-1/-2 SAR imagery acquired during the summers of 1993 and 1995 through 2000. We selected Makushin based on a small increase in microearthquake activity that occurred there during the fall and winter of 2000. Our purpose was to prospect for possible ground deformation caused by magmatic, hydrothermal, or tectonic processes, in a fashion similar to recent investigations at Westdahl volcano [*Lu et al.*, 2000b], Akutan Island [*Lu et al.*, 2000c], and Mount Peulik volcano [*Lu et al.*, 2002]. We discovered that ~7 cm of uplift centered on the eastern flank of the volcano occurred between 1993 and 1995, at least 5 years before the recent increase in seismic activity. In hindsight, the uplift was probably associated with an unsubstantiated report of an eruption in 1995. We also mapped interferometric coherence over different time intervals and compared the coherence maps with an optical satellite

[1]U.S. Geological Survey, EROS Data Center, Raytheon ITSS, Sioux Falls, South Dakota, USA.
[2]U.S. Geological Survey, Alaska Volcano Observatory, Anchorage, Alaska, USA.
[3]Oregon Department of Geology and Mineral Industries, Baker City, Oregon, USA.
[4]U.S. Geological Survey, Menlo Park, California, USA.
[5]U.S. Geological Survey, David A. Johnston Cascades Volcano Observatory, Vancouver, Washington, USA.

0148-0227/02/2001JB000970$09.00

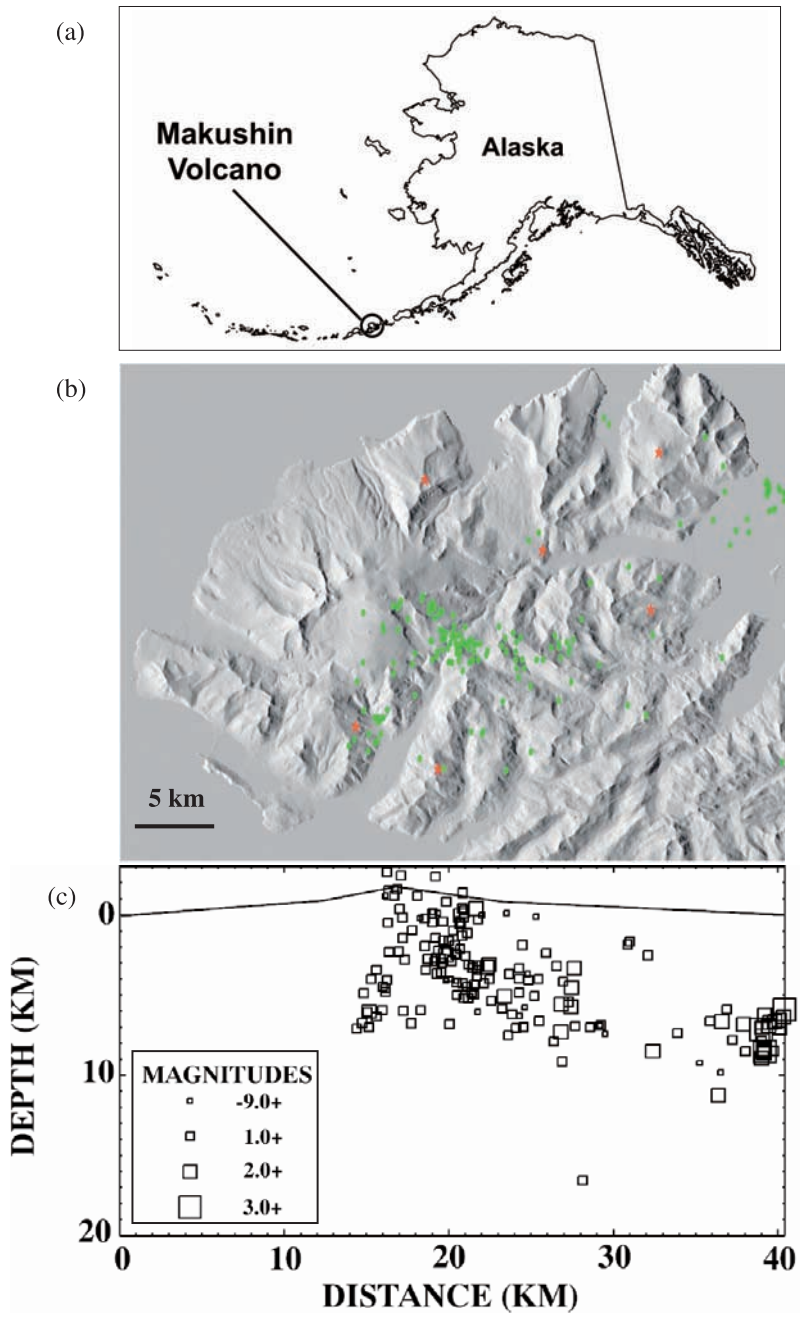

Figure 1. (a) Map showing the location of Makushin Volcano on north Unalaska Island in the central Aleutian arc, Alaska. (b) Earthquake epicenters (green circles) from July 1996 through August 2000 as located by a local seismic network (red stars) operated by the Alaska Volcano Observatory. (c) Cross section (west to east) of earthquakes shown in Figure 1b.

image, air photos, and a geologic map of the Makushin volcanic field to evaluate the effectiveness of C band (wavelength of 5.7 cm) InSAR at high-latitude volcanoes. This result should provide useful guidance for InSAR research at similar volcanoes in the Aleutians and elsewhere.

1.1. Makushin Volcano: Setting and Historical Activity

[4] Makushin is a broad, truncated stratovolcano, 1800 m high and 16 km in basal diameter, located in the central Aleutian volcanic arc of Alaska (Figure 1). A breached summit caldera 3 km across contains a small cinder cone, eroded remnants of other cones, and several active fumaroles. The volcano is capped by an ice field, and subsidiary glaciers descend the larger flanking valleys. The edifice was constructed during two distinct periods of volcanism starting in Pliocene or early Pleistocene time [*Drewes et al.*, 1961]. The Pleistocene lavas are dominantly basalt and basaltic andesite but include some andesite and dacite [*Drewes et al.*, 1961; *Nye*, 1990]. Early Holocene lavas have a wide compositional range and are generally more silicic than the Pleistocene lavas. Late Holocene lavas mark a return to more mafic compositions [*Miller et al.*, 1998].

Makushin sits ~28 km west of the town of Unalaska/Dutch Harbor, the largest population center in the Aleutian islands and the principal fishing, shipping, and air transportation hub for westernmost Alaska [*Beget et al.*, 2000].

[5] During historical time Makushin has been one of the more active volcanoes in the Aleutians, producing at least 17 explosive eruptions since the late 1700s [*Miller et al.*, 1998; *McConnell et al.*, 1997]. Geologic studies suggest that larger explosive eruptions occurred more than two dozen times during the last several thousand years, depositing widespread ash layers. In addition, a series of very large eruptions ~8000 to 8800 years ago produced the present summit crater and generated numerous pyroclastic flows and surges, a debris avalanche, and lateral blast [*Beget et al.*, 2000; *McConnell et al.*, 1997].

[6] During the past 300 years the recorded eruptions of Makushin have been relatively small with a volcanic explosivity index (VEI) of 1–3 [*Simkin and Siebert*, 1994]. They typically sent ash columns 3–10 km above the volcano's summit and deposited small amounts of ash on the flanks [*Miller et al.*, 1998]. Additional smaller eruptions probably occurred during this period but were unrecorded, either because they occurred when the volcano was obscured by clouds or because the eruptive products did not extend beyond the volcano's flanks. *Simkin and Siebert* [1994] reported small explosive eruptions (VEI 1) from the summit in 1980 and 1987, and a strong steam plume that did not contain ash in 1986. *Beget et al.* [2000, p. 6] reported "In 1983 volcanic explosions were heard by nearby geologists but never correlated with specific deposits, and in 1996 ash deposits found at the summit and on the volcano's flanks were probably produced by a previously undocumented eruption in 1995 [*McConnell et al.*, 1997]".

1.2. Observations of the January 1995 Eruption, Its Products, and Effects

[7] To follow up the possibility of an eruption during the mid 1990s [*Beget et al.*, 2000; *McConnell et al.*, 1997] that might correlate with the uplift detected with InSAR (see section 2.1), we conducted a comprehensive search of all available information for reports of eruptive activity at Makushin between 1993 and 2000. *Neal et al.* [1996] reported possible phreatic explosions on 14 and 23 September and 5 November 1993, based on aircraft pilot reports of possible ash clouds above the volcano, a sulfurous smell, and a dark discoloration of snow near the volcano's summit. *Neal et al.* [1995] and records at the Alaska Volcano Observatory (AVO) contain a 14 January 1994 pilot report of a small eruptive cloud rising ~1000 m above the volcano.

[8] The most notable reports are from 30 January 1995, when a small steam and ash cloud were noted by a U.S. Coast Guard C-130 at 2046 UT (1246 Alaska Standard Time). It rose to altitudes of ~2400 m and was carried northeast by prevailing winds. This observation was confirmed by a second pilot report of a plume of "steam and ash" ~300 m above the volcano at 2225 UT [*McGimsey and Neal*, 1996; *Smithsonian Institution*, 1995]. An AVHRR image acquired at 2245 UT, two hours after the first report, revealed nothing clearly related to an eruption. Likewise, AVHRR images at 2009 UT on 30 January and 0040 UT on 31 January showed nothing unusual (K. Dean, AVO, personal communication, 2001). Taken together, these observations suggest that the 30 January 1995 eruption was small and lasted for only a few hours. No similar or stronger activity at Makushin has been reported since (T. Neal, personal communication, 2001).

[9] During a geologic mapping field survey conducted in the summer of 1996, observers noted a thin layer of ash trapped in snow on the upper south flank of Makushin, and also ash, lapilli, and breadcrust bombs covering the summit area. The deposits presumably appeared at the surface when seasonal snow melted away [*McConnell et al.*, 1997]. Petrographic and geochemical analyses of the ash revealed juvenile glass, accretionary lapilli, and clasts of basaltic lava, suggesting a recent phreatomagmatic eruption that probably correlates with the activity reported in January 1995 [*Roach and McConnell*, 1996]. Figures 2a and 2b show two photos, one taken in July 1994 and the other in August 1996. The small steam vent in the 1994 image (Figure 2a) has enlarged to a cinder cone with a steep-sided crater (Figure 2b). The brown discoloration of the snow in Figure 2b resulted from a thin surge deposit and ashfall that apparently affected only the upper snowfields of the volcano. Figure 2c is an oblique air photo taken in August 1996, giving a close look of the crater outlined in Figure 2b. The un-eroded, steep-sided asymmetric crater ~50 m across with a sulfurous lake inside had not been observed during previous field surveys. We surmise that changes in morphology of the summit area resulted from the eruptive activity in January 1995.

1.3. Seismic Observations

[10] A local seismic network comprising six short-period instruments was installed on Makushin in July 1996. From July 1996 to August 2000, 176 earthquakes were located near the volcano (Figure 1b). All of the events were relatively small, with local magnitudes of 0.1 to 3.2. Hypocentral depths range from 2 km above sea level to 15 km below (Figure 1c). Most of the hypocenters fall into one of two prominent clusters. The larger and more active cluster is centered ~6 km southeast of the volcano's summit and includes earthquakes that range in-depth from 2 to 9 km (Figures 1b and 1c). The second cluster is centered ~24 km east of the summit of Makushin, beneath Unalaska Bay, at depths of 6 to 14 km (Figures 1b and 1c). The average rate of occurrence for earthquakes near Makushin is 2–3 shocks per month. A minor increase of 56 earthquakes occurred during May–June 1997, with events in both hypocentral clusters. A more sustained increase at comparable levels of activity began in July 2000 and lasted till May 2001.

1.4. InSAR Studies of Volcanoes

[11] Since its first application to an active volcano at Mount Etna, Italy [*Massonnet et al.*, 1995], InSAR has become an important geodetic imaging tool for studying volcanoes worldwide [e.g., *Massonnet and Feigl*, 1998; *Zebker et al.*, 2000]. Simply stated, InSAR combines phase information from two or more SAR images of the same area acquired from similar vantage points at different times to produce an interferogram. The interferogram, which shows range changes in the satellite look direction between the satellite and the ground, can be further processed with a digital elevation model (DEM) to image ground deforma-

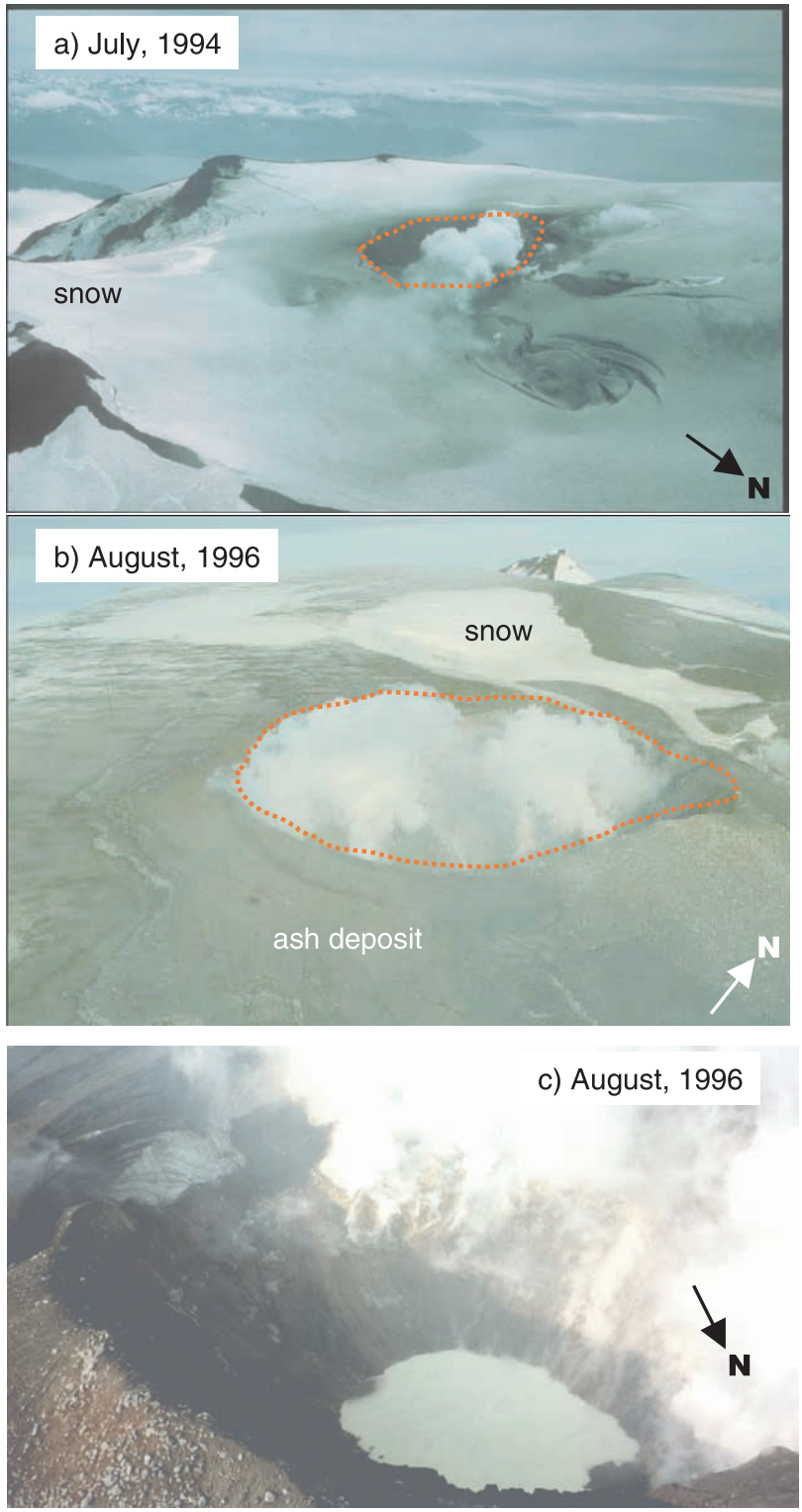

Figure 2. (a) An oblique air photo taken in July 1994, showing the central summit area of Makushin Volcano. (b) An oblique air photo taken in August 1996, showing morphologic changes in the vent area that probably occurred during an eruption on 30 January 1995. The brown area in Figure 2b is a deposit of volcanic ash and bombs. (c) An oblique air photo taken in August 1996 gives a close look at the crater outlined in Figure 2b. In the upper left part of the image, lighter and darker bands correspond to snow and ash layers. The steep-sided, asymmetric crater ~50 m across with a lake inside was not observed during previous field surveys, suggesting that it was produced during the January 1995 eruption.

Table 1. Interferometric Data Acquisition Parameters[a]

Orbit 1	Orbit 2	Date 1	Date 2	Track	Frame	h_a, m	Figure
E1_10967	E2_07670	20 Aug. 1993	10 July 1996	301	2518	1859	3b and 5a
E1_11239	E2_12451	8 Sept. 1993	6 Sept. 1997	72	2518	−817	3c and 5d
E1_10738	E1_21603	4 Aug. 1993	1 Sept. 1995	72	2518	−59	3d
E1_10738	E2_07441	4 Aug. 1993	21 Sept. 1996	72	2518	−66	3e
E1_11740	E2_22104	13 Oct. 1993	6 Oct. 1995	72	2518	−275	3f
E1_21603	E2_07441	1 Sept. 1995	21 Sept. 1996	72	2518	610	4a
E2_07670	E2_13181	7 Oct. 1996	27 Oct. 1997	301	2518	−118	4b
E2_23202	E2_27720	27 Sept. 1999	7 Aug. 2000	301	2518	−56	4c
E2_06668	E2_23201	29 July 1996	27 Sept. 1999	301	2518	108	4d
E2_17690	E2_27710	7 Sept. 1998	7 Aug. 2000	301	2518	129	4e
E1_11238	E1_11740	8 Sept. 1993	13 Oct. 1993	72	2518	−41	4f
E1_10739	E1_11239	4 Aug. 1993	8 Sept. 1993	72	2518	20	

[a] The parameter h_a is the altitude of ambiguity.

tion at a horizontal resolution of tens of meters over areas of ~100 km × 100 km with centimeter to sub-centimeter precision under favorable conditions [e.g., *Massonnet and Feigl*, 1998; *Rosen et al.*, 2000]. InSAR has proven to be an effective tool for mapping ground deformation at several active volcanoes and restless calderas [e.g., *Amelung et al.*, 2000; *Beauducel et al.*, 2000; *Lu et al.*, 2000a, 2000b, 2000c, 2002; *Massonnet et al.*, 1995; *Sigmundsson et al.*, 1999; *Vadon and Sigmundsson*, 1997; *Wicks et al.*, 1998].

2. InSAR Deformation Observations, Modeling, and Coherence Analysis

[12] We used the two-pass InSAR method [*Massonnet and Feigl*, 1998; *Rosen et al.*, 2000] with 17 images that were acquired by the European Space Agency (ESA) ERS-1 and ERS-2 satellites and provided to us by the Alaska SAR Facility (ASF) (Table 1). The images, from the summers of 1993 and each year from 1995 to 2000, were selected to minimize the loss of radar coherence due to snow and ice [*Lu and Freymueller*, 1998]. No SAR data were acquired during the summer of 1992 (from June to October). Also, ERS-1 was maneuvered for a different purpose from April 1994 to March 1995, resulting in no useful data for InSAR applications during summer 1994 (i.e., data acquired during this period cannot be combined with those from other time periods to produce useful interferograms). The SAR images used in this study were from two different descending tracks, 301 and 72 (Table 1). In each case, the satellites traveled southward along the direction S13°W over Makushin and looked westward (the SAR sensors onboard the ERS-1/ERS-2 satellites are side-looking radars). The look angles over the center of Makushin were about 25° and 20° from vertical for tracks 301 and 72, respectively.

[13] We used the U.S. Geological Survey's (USGS) 15-minute Alaska DEM for our analysis. The DEM has a horizontal grid spacing of ~60 m, a specified horizontal accuracy of ~60 m and root-mean square vertical error of ~15 m [U. S. Geological Survey, 1993]. Similar to the methodology described by *Lu et al.* [2002] in their InSAR study of Mount Peulik, Alaska, we first verified the overall accuracy of the DEM using a pair of radar images of the Makushin area acquired on 4 August and 9 September 1993 (Table 1). The altitude of ambiguity, h_a, for this image pair is ~20 m, which means that a DEM error of that magnitude would produce one interferometric fringe in an interferogram formed from these two images. No fringes were evident in the 1993 interferogram. The interferograms used for our deformation analysis have values of h_a ranging from 41 m to 1859 m, making them less sensitive to topography than the 1993 interferogram. We concluded that the overall accuracy of the Makushin DEM is within specifications. For an interferogram with $h_a > 100$ m, the uncertainty in observed deformation due to the DEM error is less than 15% of one fringe. Therefore, any topographic artifacts in our other interferograms are negligible.

2.1. InSAR Deformation Observations of Makushin

[14] We generated 11 interferograms of Makushin that collectively span the time interval from August 1993 to October 2000 (Figures 3 and 4). The time separation of image pairs ranges from 35 days to 4 years. Examination of the interferograms demonstrates that C band interferometric coherence persists for at least 3 years over most of the study area (see section 2.3 for detailed discussion of interferometric coherence). Each interferometric fringe (i.e., red-blue color cycle) in Figures 3–5 corresponds to a range change of 2.83 cm (half of ERS-1/ERS-2 radar wavelength) in the satellite look direction. In cases where less than one complete fringe is discernible in areas of good coherence, we concluded that no significant deformation occurred during the corresponding time interval. No conclusion can be drawn for areas with poor coherence, such as the snow-and-ice covered summit area.

[15] The terrain surrounding Makushin is very rugged (Figure 3), which causes severe geometric distortion in SAR images (foreshortening, layover, or shadowing) [*Curlander and McDonough*, 1991] in parts of the study area. These areas correspond to dark areas in Figures 3–5. All the interferograms presented in this paper were geocoded (i.e., referenced to map coordinates). Terrain-induced distortions were either corrected where the terrain slope is less than the radar look angle, or masked where slope is close to or greater than the radar look angle.

[16] Ground deformation corresponding to more than two fringes (~7 cm) was observed in the interferograms that span the periods from 20 August 1993 to 7 October 1996 (Figure 3b); from 8 September 1993 to 6 September 1997 (Figure 3c); from 4 August 1993 to 1 September 1995 (Figure 3d); from 4 August 1993 to 21 September 1996 (Figure 3e); and from 13 October 1993 to 6 October 1995 (Figure 3f). No significant deformation was observed in the interferograms that span the periods from 1 September 1995 to 21 September 1996 (Figure 4a); from 7 October 1996 to 27 October

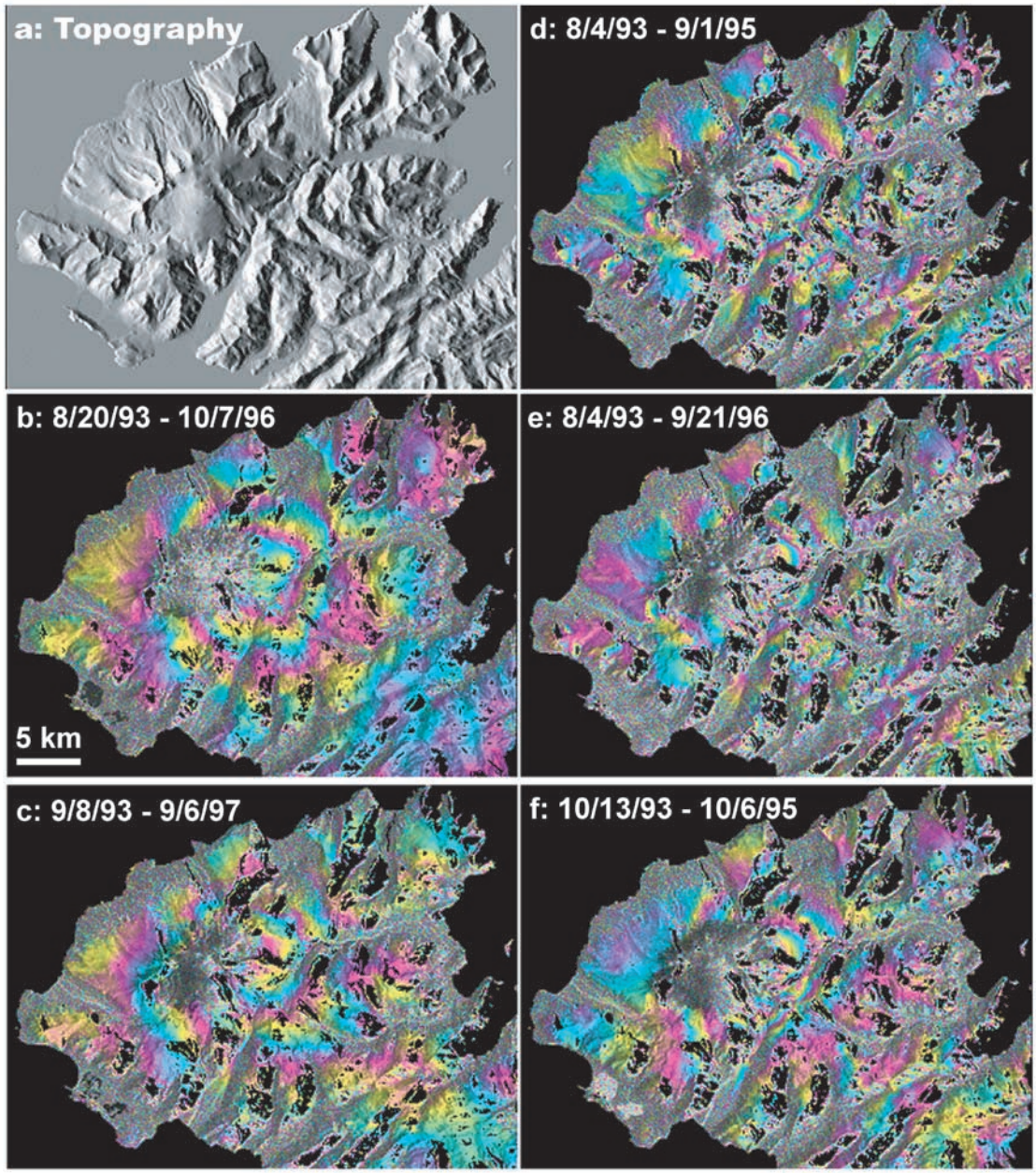

Figure 3. (a) Shaded-relief map of Makushin produced from the USGS Alaska DEM, illustrating the rugged terrain over the volcano. Topography-removed interferograms for the periods from (b) 20 August 1993 to 7 October 1996 (h_a = 1859 m); (c) 8 September 1993 to 6 September 1997 (h_a = −817 m); (d) 4 August 1993 to 1 September 1995 (h_a = −59 m); (e) 4 August 1993 to 21 September 1996 (h_a = −66 m); and (f) 13 October 1993 to 6 October 1995 (h_a = −275 m). Each interferometric fringe (full color cycle) represents 2.83 cm of range change between the ground and the satellite. Surface uplift of ∼7 cm (2+ fringes) occurred between October 1993 and September 1995.

1997 (Figure 4b); from 27 September 1999 to 7 August 2000 (Figure 4c); from 29 July 1996 to 27 September 1999 (Figure 4d); from 7 September 1998 to 7 August 2000 (Figure 4e); and from 8 September 1993 to 13 October 1993 (Figure 4f). In short, all of the interferograms that span October 1993 to September 1995 show uplift corresponding to 2–3 fringes, and all of the interferograms that exclude this period show essentially no deformation.

[17] Figure 3b shows the interferogram for the period from 20 August 1993 to 7 October 1996, which includes a fringe pattern reflecting surface uplift by ∼7 cm. This interferogram has the largest h_a (1859 m) of the group (Table 1), which means that any plausible errors in the DEM have negligible effect. The images used for this interferogram are from track 301, which has a radar look angle of 25° over the center of the volcano. Consequently, this interferogram is less affected by terrain-induced distortion (i.e., less gaps) than those produced from track 72 images, which have a look angle of 20° (Table 1). The fringes in Figure 3b are corroborated by similar patterns in independ-

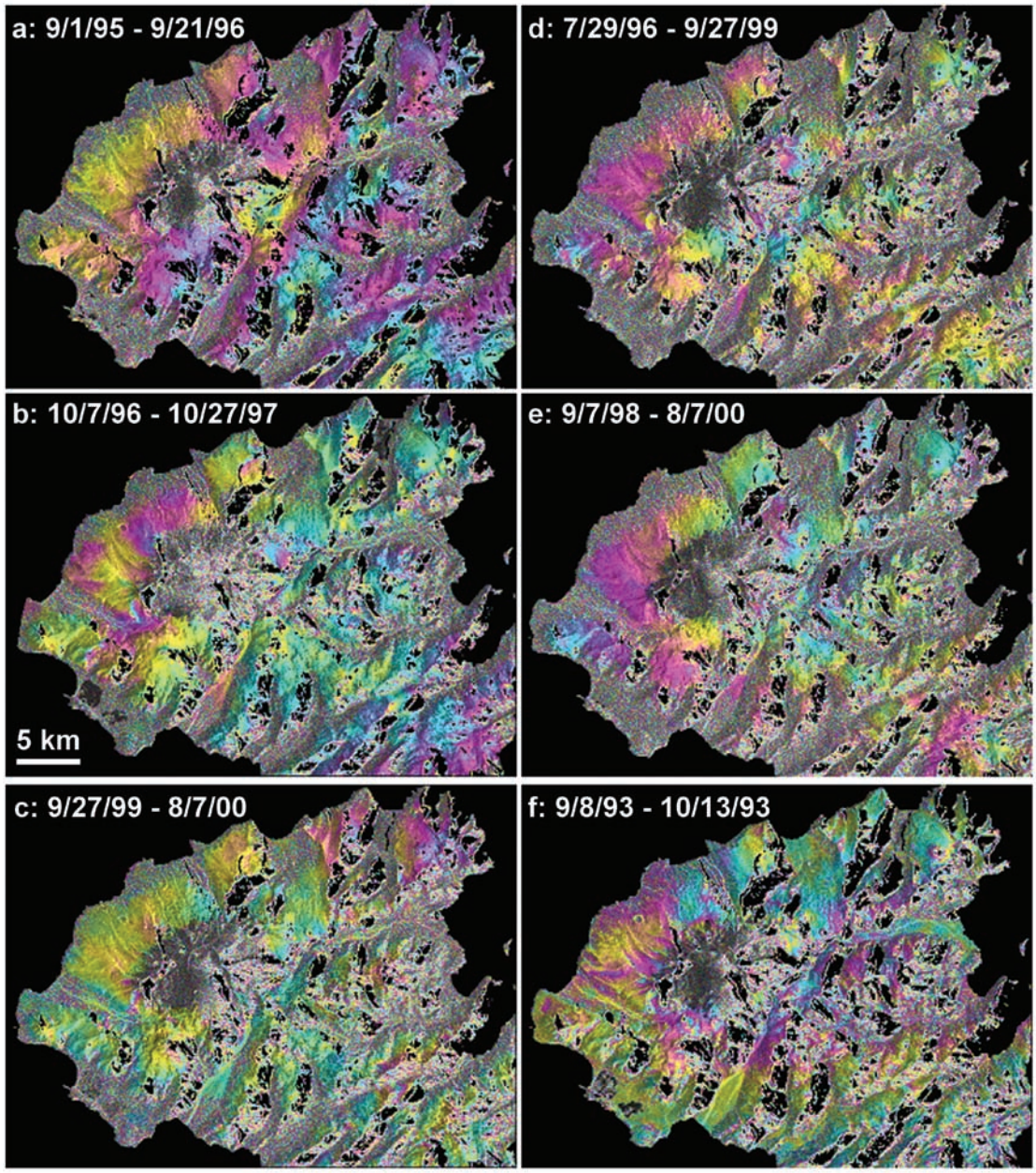

Figure 4. Topography-removed interferograms for the periods (a) from 1 September 1995 to 21 September 1996 (h_a = 610 m); (b) from 7 October 1996 to 27 October 1997 (h_a = −118 m); (c) from 27 September 1999 to 7 August 2000 (h_a = −56 m); (d) from 29 July 1996 to 27 September 1999 (h_a = 108 m); (e) from 7 September 1998 to 7 August 2000 (h_a = 129 m); and (f) from 8 September 1993 to 13 October 1993 (h_a = −41 m). No significant deformation was detected during these time intervals.

ent interferograms acquired from track 72, with different acquisition dates and different h_a (Figures 3c–3f). This assures us that the observed fringes represent primarily ground deformation, rather than DEM errors or atmospheric delay anomalies.

2.2. InSAR Deformation Modeling

[18] We modeled the observed deformation pattern (Figures 3b–3f) using a Mogi source embedded in an elastic homogeneous half-space [*Mogi*, 1958; *McCann and Wilts*, 1951]. The four parameters used to describe the Mogi source are horizontal location (easting x, northing y), depth d, and volume change ΔV. To account for topographic effects, we adopted a simple approach proposed by *Williams and Wadge* [1998] in which the elevation of the reference surface varies according to the elevation of each computation point in the model. We used a nonlinear least squares inversion approach to optimize the source parameters [*Press et al.*, 1992].

[19] We first modeled the interferogram from track 301 (Figure 3b). This interferogram is superior to those from track 72 (Figures 3c–3f), because the altitude of ambiguity for the former is much greater (Table 1). For the same reason, the track 301 interferogram is generally more coherent. Also, the smaller SAR look angle for track 72

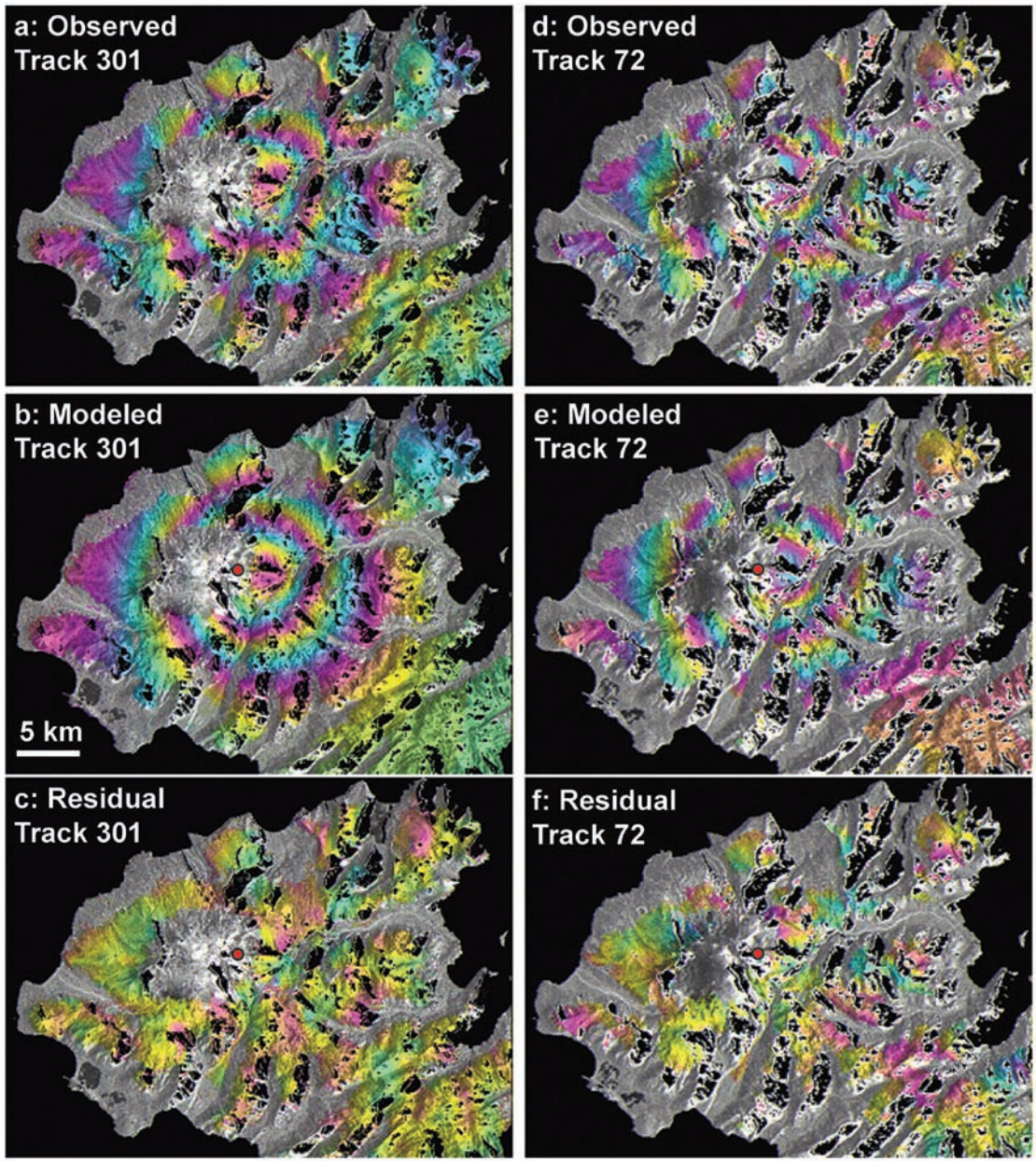

Figure 5. (a) Observed, (b) best fit synthetic, and (c) residual interferograms of Makushin for the period from 20 August 1993 to 7 October 1996. Images used are acquired from track 301. (d) Observed, (e) best fit synthetic, and (f) residual interferograms for the time interval between 8 September 1993 and 6 September 1997. Images are from track 72. Each fringe (full color cycle) represents 2.83 cm of range change between the ground and the satellite. The synthetic interferograms were produced using the corresponding best fit Mogi sources (red circle in Figures 5b, 5c, 5e, and 5f). Areas lacking interferometric coherence are uncolored.

images (20° versus 25°) results in greater geometric distortion and therefore less areas of useful information (note the greater proportion of dark areas in Figures 3c–3f relative to Figures 3b). The synthetic interferogram with the best fitting model parameters is shown in Figure 5b and the residual interferogram, which shows the difference between the observed and modeled interferograms, is shown in Figure 5c. From the residual interferogram, we can see that the Mogi source fits this observed interferogram remarkably well (variance of 20.83 mm^2). Our best model locates the inflation center beneath the east flank of Makushin, just outside the caldera. The x and y positions, with respect to the lower left corner of the interferogram (Figure 5), are 18.30 ± 0.13 km and 16.16 ± 0.12 km, respectively. The presumed magma body was located at a depth of 6.80 ± 0.28 km below sea level. The surface uplift volume corresponds to a source volume increase of 0.022 ± 0.002 km^3, assuming Poisson's ratio of 0.25.

[20] We then modeled the interferogram shown in Figure 3c, which has the largest altitude of ambiguity among the

track 72 interferograms (Figures 3c–3f). Modeling this interferogram yielded model parameters for the point source that are similar to those for the interferogram from track 301 ($x = 18.57 \pm 0.19$ km, $y = 16.38 \pm 0.17$ km, $d = 7.00 \pm 0.39$ km, $\Delta V = 0.024 \pm 0.003$ km^3, and variance = 23.29 mm^2). Even though uncertainties and variance of model parameters are slightly larger than those for the track 301 interferogram (Figure 3b), the two models are essentially the same at the 95% confidence level. The synthetic and residual interferograms that correspond to the best fitting model for interferogram in Figure 3c are shown in Figures 5e and 5f. Modeling of the other interferograms from track 72 (Figures 3d–3f) produced similar results but both uncertainties of model parameters and variances of the best fitting models are larger.

[21] No significant volcano-wide deformation was observed in the interferograms that do not span the period from 13 October 1993 to 1 September 1995 (Figures 4a–4f). However, slight or localized deformation might have gone undetected owing to loss of coherence in the summit area as a result of glacier ice or severe geometric distortion in many parts of the study area.

2.3. Correlation of InSAR Coherence With Geology, Landsat 7 Image, and Air Photos

[22] In order for useful information to be derived from an interferogram, the radar returns must be phase coherent [e.g., *Lu and Freymueller*, 1998; *Zebker and Villasenor*, 1992]. In general, the types of surface material and vegetation cover are the most important factors affecting interferometric coherence [e.g., *Lu and Freymueller*, 1998; *Wegmuller and Werner*, 1997]. Thus, the ability of InSAR to measure volcano deformation depends on the persistence of phase coherence over appropriate time intervals on various types of volcanic deposits with various types of vegetation cover.

[23] To make a qualitative assessment of interferometric coherence at Makushin, we generated binary coherence images for 3 time intervals. By inspection, we classified parts of the images in two categories: a) coherent, where useful deformation can be derived, and b) noncoherent, where no useful information can be extracted. Figures 6a–6c show coherence images for time intervals of 3 years, 1 year, and 35 days, respectively. Yellow and light blue are used to represent coherent and noncoherent areas, respectively.

[24] To classify vegetation cover, we obtained multispectral satellite images acquired on 18 September 2000 by Landsat 7 [*NASA*, 1999]. Landsat 7 acquires images at visible, near infrared, and thermal wavelengths, and therefore is very useful for determining the character of vegetation. We co-registered the Landsat 7 images with the interferograms shown in Figures 3–5, and then created a color-composite image by assigning bands 5, 4, and 3 to red, green, and blue, respectively. Band 5 is in the near-infrared part of the spectrum (1.55–1.75 μm), which is sensitive to the moisture content of soil and vegetation [*Sabins*, 1997]. Band 4 is another near-infrared channel (0.76–0.90 μm) and is useful for mapping biomass content. Band 3 is a visible channel (0.63–0.69 μm) that is sensitive to chlorophyll absorption and helps to discriminate among vegetation types. In Figure 6d, bright blue areas represent ice and snow, which occurs primarily on the upper portions of Makushin Volcano. Pink and white bands represent clouds over the northeast and southeast parts of the island. Sparsely vegetated areas such as young lava flows and rocky high alpine areas are shown in purple, whereas relatively densely vegetated areas are in green. In general, vegetation at higher elevations consists mainly of short grass or sparsely distributed tall grass whereas at lower elevation areas it is densely distributed tall grass. The grass species at lower elevation consist of a plant community that is primarily reed grasses, sedges, and low growing forbs. The grass species at higher elevation are similar to but do not grow as tall and dense as those at lower elevation and consist of little or no bush or forbs. To give a sense of the vegetation, we show an area of vegetated lava flows on the northwest flank of Makushin in Figure 7a. Figures 7b and 7c show the type of short grass and sparsely distributed tall grass, respectively, that thrive on lava and rocky surfaces. In Figure 7c, bare surface appears pink or purple. Figure 7d shows typical dense tall grass on Makushin Island. In general, the short grass is less than 20 cm high, and tall grass can be as much as 1 m high.

[25] To further evaluate the surface materials at Makushin, we also present a simplified version of a geologic map modified from *Miller et al.* [1998] (Figure 6e). The surface consists mainly of alluvium deposits (A), postcaldera basalt and andesitic flows and scoria (L), precaldera basalt and andesite flows (PL), granodiorite batholith (GB), sedimentary rocks (SR), pyroclastic deposits (P), and ice (I).

[26] Inspection of Figures 6a–6e leads us to make the following observations:

1. In areas covered by sparsely vegetated lava flows and rocks, interferometric coherence is maintained well enough for deformation mapping over time periods of more than 3 years. Coherence after 3 years (Figure 6a) is not significantly less than after 1 year (Figure 6b). Similarly, most of the pyroclastic deposits (P in Figure 6e) remain coherent for at least 1 year and up to 3 years, although in this case 1-year coherence is slightly better than 3-year coherence. In areas covered by lava and rocks with dense tall grass, interferometric coherence for 1 year is slightly better than for 3 years, but both are significantly worse than for 35 days. Areas covered by alluvium are significantly more coherent after 35 days (Figure 6c) than after 1 year or 3 years, which suggests that alluvium surfaces maintain coherence only for several months within the same summer. These observations are similar to those of *Lu and Freymueller* [1998] for the Katmai volcano group on the Alaska Peninsula.

2. Ice and snow surfaces lose coherence very rapidly. The glaciated summit area of Makushin lost coherence in less than 35 days (Figure 6c). This is consistent with a loss of coherence observed at Westdahl volcano over a 3-day period [*Lu et al.*, 2000b]. Therefore, snow and ice-covered areas pose a significant problem for volcano deformation studies, especially if the deforming area does not extend beyond snow and ice to areas that maintain coherence for longer periods.

3. Most of the surface surrounding Makushin Volcano is vegetated, but coherence persists there for periods of months to more than 3 years. Vegetation is generally less well developed on lava flows than on alluvium or pyroclastic deposits (Figures 6d and 6e). We expected and found that coherence was maintained for more than 3 years on nonvegetated lava surfaces, as reported by *Lu and*

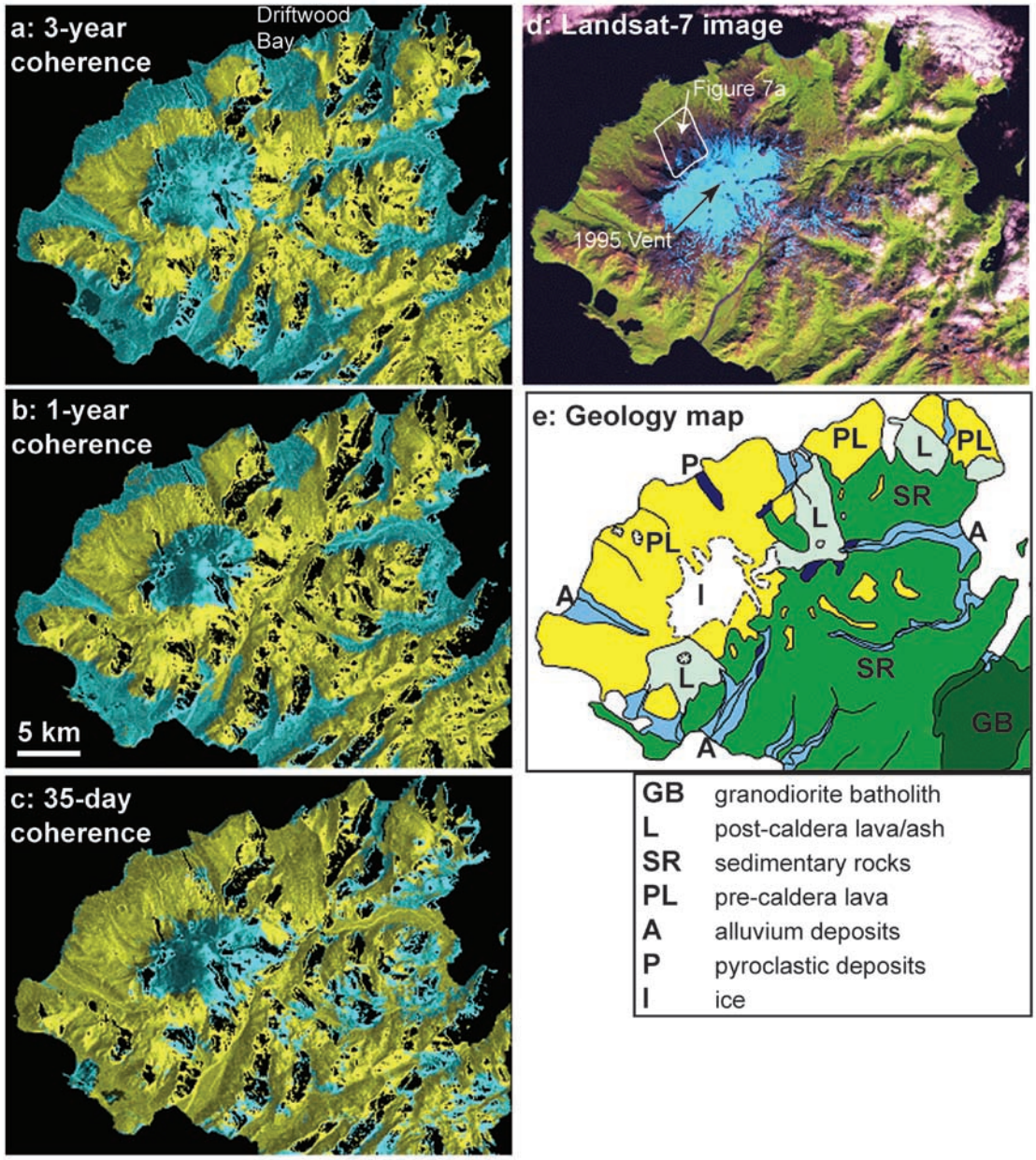

Figure 6. Qualitative interferometric coherence maps of Makushin Volcano that span (a) 3 years (20 August 1993 to 7 October 1996), (b) 1 year (1 September 1995 to 21 September 1996), and (c) 35 days (8 September 1993 to 13 October 1993). Yellow indicates areas where coherence is maintained and information on ground deformation, if any, can be retrieved. Light blue indicates areas where coherence is lost, and black indicates areas of severe geometric distortion. (d) A color composite of Landsat 7 images created from bands 5, 4, and 3 as red, green, and blue channels, respectively. The outlined area shows the position where the photo in Figure 7a was taken. (e) Simplified geologic map of Makushin Volcano, modified from *Miller et al.* [1998]. The surface consists mainly of alluvium deposits (A), postcaldera basalt and andesitic flows and scoria (L), precaldera basalt and andesite flows (PL), granodiorite batholith (GB), sedimentary rocks (SR), pyroclastic deposits (P), and ice (I).

Freymueller [1998]. On the other hand, we were surprised to find that coherence was also maintained for a similar period on lava and rocky surfaces that are vegetated. The fact that good coherence was maintained for 35 days in areas covered by sparse tall grass was also surprising. This indicates that C band radar penetrates short grass and sparse tall grass to reach the surface. Short and tall grass are the predominant vegetation covers at most Aleutian and other sub-arctic volcanoes, so our results are encouraging that InSAR will be effective not only throughout the Aleutians but also in other high-latitude regions, including the Kamchatka and Kurile volcanic arcs.

4. For surfaces with densely distributed tall grass, C band coherence is lost in several months within the same summer

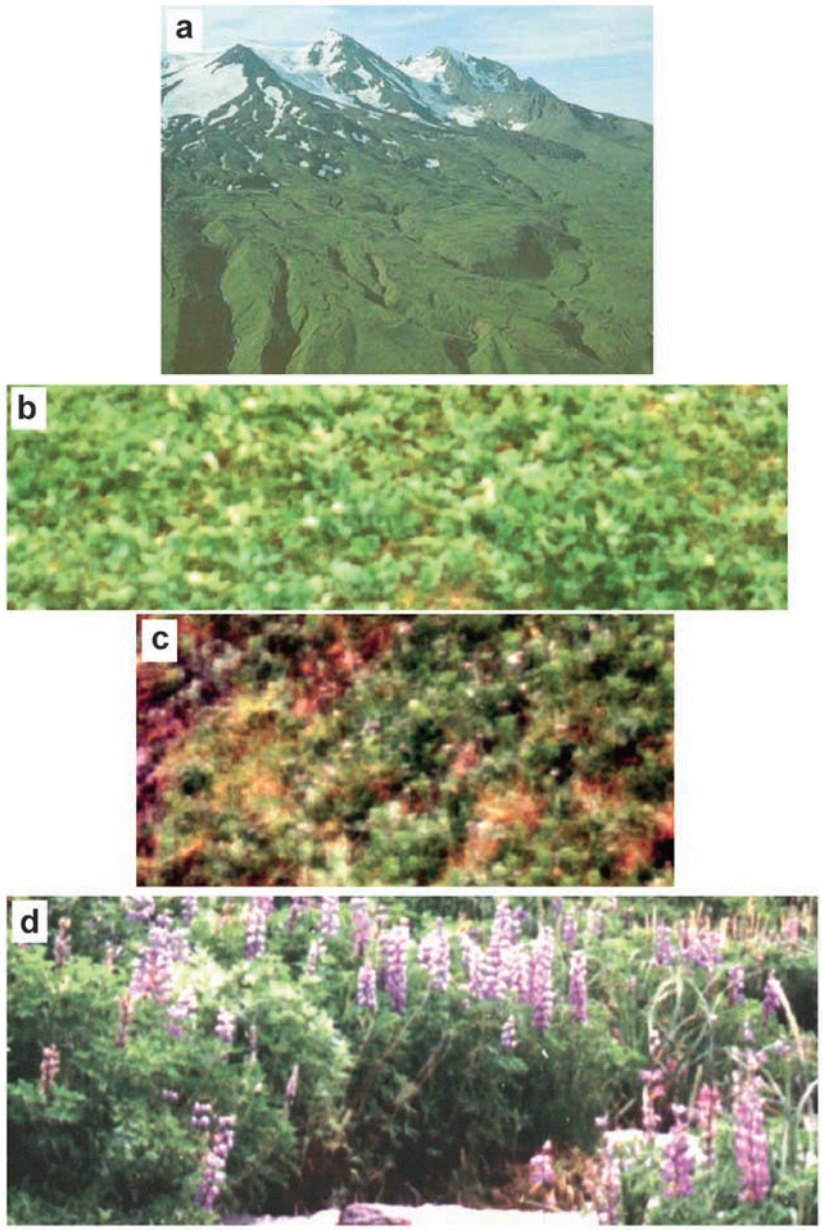

Figure 7. (a) Photo taken in August 1996 showing vegetated lava flows on the northwest flank of Makushin Volcano (area outlined in Figure 6d). The arrow in Figure 6d shows the direction from which the picture was taken. (b) Photo taken in August 1996 to illustrate the type of short grass that covers lava flows at higher elevations. (c) Photo taken in August 1996 to illustrate the type of sparsely distributed tall grass that covers lava flows at higher elevations. (d) Photo taken in August 1996 to illustrate the type of densely distributed tall grass at lower elevation areas. In general, the short grass is less than 20 cm high, and tall grass can be as much as 1 m high. The areas shown in Figures 7c–7d are ~5 m wide on the ground.

regardless of surface types. For example, lava flows and rocky surfaces near the shore maintain coherence in the 35-day interferogram (Figure 6c), but not in the 1-year or 3-year ones (Figures 6a and 6b). For sparsely vegetated surfaces, on the other hand, the most significant factor that affects interferometric coherence at Makushin seems to be the type of surface material. In this case, vegetation also affects coherence, but to a much smaller degree. For example, in the Driftwood Bay area, alluvium supports considerably less vegetation than postcaldera lavas to the south, but 1-year coherence is much better over the lavas than over the alluvium (Figure 6b).

5. The ash from the January 1995 eruption is not observable from either SAR amplitude images or interferometric coherence maps. Most of the ash deposited over the snow/ice area at the volcano summit. Changes in SAR images due to changes in snow/ice are far more than those due to ash deposits. Therefore, the ash from January 1995

eruption is not discernable from SAR images or coherence maps.

3. Discussion

[27] Using five separate radar interferograms, we found that ~7 cm of surface uplift occurred at Makushin Volcano between October 1993 and September 1995. This uplift, centered ~5 km east of the volcano's summit, could have been caused by a volume increase of ~0.022 km^3 at a depth of ~7 km below sea level. We cannot determine precisely how various eruptive events at Makushin during 1993–95 relate to the 7 cm of uplift revealed by interferograms that span that period. The most likely scenario, in our opinion, is that the observed uplift was caused mainly by the accumulation of magma that fed the eruption of 30 January 1995. We favor that interpretation because field observations of several eruptive events during 1993–1995 suggest that the 30 January 1995 event was the largest. It resulted in significant changes in the vent and crater area and deposited measurable amounts of ash on the upper flanks of the volcano [*McConnell et al.*, 1997]. Similar effects were not observed following eruptions in 1993 or 1994. Consistent with this idea, an interferogram for the 35-day period from 9 September 1993 to 13 October 1993 (Figure 4f), which included eruptions on 14 and 23 September, shows no significant volcano-wide deformation.

[28] The interferograms show no evidence of subsidence associated with the 30 January 1995 event, but a small amount could be masked by net uplift. Specifically, an interferogram spanning the period from 4 August 1993 to 1 September 1995 (including the event) shows ~7 cm of net uplift, whereas an interferogram spanning the period from 1 September 1995, to 21 September 1996 (following the event) shows essentially no deformation (Figures 3d and 4a, respectively). Maximum uplift during the first period might have been greater than ~7 cm and partly offset by an unknown amount of syneruptive or posteruptive subsidence. However, any subsidence that might have occurred had ended by 1 September 1995, as evidenced by the second interferogram.

[29] The volume of eruptive products from the 30 January 1995, event is unknown, so any comparison to the source volume change determined here is purely conjectural. However, the small size (VEI 1) of Makushin eruptions in 1980 and 1987 [*Simkin and Siebert*, 1994] and field reports of a relatively small steam and ash cloud above the volcano on 30 January 1995, seem consistent with the relatively small source volume change derived from the interferograms.

[30] The center of uplift at Makushin is offset by ~5 km from the eruptive vent (Figure 5), which is roughly coincident with the most active cluster of seismic activity observed between 1996 and 200 (Figure 1b). This is reminiscent of the InSAR observation of volcanic deflation associated with the 1997 eruption at Okmok volcano, a basaltic shield located ~45 km southwest of Makushin [*Lu et al.*, 2000a]. In that case, too, the deformation center and eruptive vent were separated by ~5 km. Similar occurrences have been reported at other basaltic shields including Kilauea and Piton de la Fournaise, and recently at the silicic Three Sisters volcanic center in the central Oregon Cascade Range [*Wicks et al.*, 2002]. In the latter case, ~10 cm of uplift that occurred mostly during 1998–2000 was centered ~5 km west of South Sister volcano, in an area that last produced an eruption ~1500 years ago.

[31] The reasons for such offsets undoubtedly vary. At basaltic volcanoes, lateral transport of magma through a rift zone, propagating dike, or lava tube can easily explain kilometer-scale offsets between a deformation center and eruptive vent. The explanation is less apparent at more silicic centers such as Katmai, Alaska [*Hildreth*, 1991], Izu-Oshima and Usu, Japan [*Newhall and Dzurisin*, 1988], Three Sisters, Oregon [*Wicks et al.*, 2002], and Makushin. Two possibilities are (1) an inclined conduit connecting a subsurface magma reservoir to a surface vent and (2) anisotropic or inelastic crustal properties resulting in an eccentric surface deformation pattern. In the first case, a 7-km-deep magma body displaced 5 km laterally from its future vent implies a conduit that dips 35° from vertical. Field studies of eroded stratovolcanoes indicate that feeder conduits are generally near vertical, but the possibility exists that the modern Makushin magma chamber is relict from earlier eruptive activity. Makushin was constructed during two distinct periods of volcanism but radial dips of flows suggest that the same principal vent area was active during both periods [*Miller et al.*, 1998], so this possibility remains unsupported. Alternatively, rock deformation might be anisotropic or inelastic, especially near active faults. In that case, simple deformation models like the one used here would be inappropriate. On the other hand, too little is known about the rock-mechanical properties of the crust near Makushin to justify a more complicated model. The 1993–95 uplift pattern and 1996–2000 earthquake distribution suggest that Makushin's east flank is most sensitive to stresses caused by magmatic inflation. Even so, future vents will likely be located in the summit area, as they have been in the recent past.

4. Conclusions

[32] Five separate radar interferograms show that ~7 cm of surface uplift occurred at Makushin Volcano between October 1993 and September 1995. Modeling indicates that the uplift, which was centered ~5 km east of the volcano's summit, could have been caused by a volume increase of ~0.022 km^3 at a depth of ~7 km below sea level. We attribute the uplift to accumulation of magma that resulted in a small explosive eruption on 30 January 1995. These observations suggest that InSAR can be used as an effective monitoring tool at many Aleutian volcanoes from summer to summer or during a single summer. Although the terrain at Makushin is rugged and geometric distortion of radar images is severe, ground deformation of a few cm can be unambiguously identified with independent interferograms.

[33] Our comparison of surface geology, vegetation cover, and interferometric coherence as a function of time shows that less vegetated lava flows and rocky surfaces at Makushin maintain coherence at C band for periods of 3 years or more, even where covered by grass. Pyroclastic deposits can be coherent for more than 1 year. Alluvium and densely vegetated lava and rocks maintain coherence throughout a single summer. These observations suggest

that InSAR can be used to study volcano deformation throughout the Aleutian arc, and probably in the Kamchatka and Kurile arcs as well.

[34] **Acknowledgments.** ERS-1/ERS-2 SAR images are copyright © 1992–2000 ESA, and were provided by NASA/ASF. This research was supported by a NASA NRA-99-OES-10 grant (RADARSAT-0025-0056), USGS contract 1434-CR-97-CN-40274, and the USGS Volcano Hazards Program. We thank the User Service of ASF for their special efforts to provide SAR data on a timely basis; D-PAF/ESA for providing precise satellite orbit information; S. Moran, T. Masterlark, P. Briole, an anonymous reviewer, and A. Linde (Associate Editor) for very helpful and constructive reviews of the manuscript; Tina Neal for insightful discussions on eruptive activity from 1993 to 2000 at Makushin Volcano; and T. Miller, J. Begét, S. Klemperer, and B. Springer for sharing the geologic map and photos of Makushin Volcano.

References

Amelung, F., S. Jonsson, H. Zebker, and P. Segall, Widespread uplift and 'trapdoor' faulting on Galapagos volcanoes observed with radar interferometry, *Nature*, *407*, 993–996, 2000.

Beauducel, F., P. Briole, and J. Froger, Volcano-wide fringes in ERS synthetic aperture radar interferograms of Etna (1992–1998): Deformation or tropospheric effect?, *J. Geophys. Res.*, *105*, 16,391–16,402, 2000.

Beget, J. E., C. J. Nye, and K. W. Bean, Preliminary volcano-hazard assessment for Makushin Volcano, Alaska, *Rep. Invest. 2000-4*, Alaska Div. of Geol. and Geophys. Surv., Fairbanks, 2000.

Curlander, J., and R. McDonough, *Synthetic Aperture Radar, Systems and Signal Processing*, John Wiley, New York, 1991.

Dean, K., M. Servilla, A. Roach, B. Foster, and K. Engle, Satellite monitoring of remote volcanoes improves study efforts in Alaska, *Eos Trans. AGU*, *79*(35), 413, 422–423, 1998.

Drewes, H., G. D. Fraser, G. L. Snyder, and H. F. Garnett Jr., Geology of Unalaska Island and adjacent insular shelf, Aleutian Islands, Alaska, *U.S. Geol. Surv. Bull., 1028-S*, 583–676, 1961.

Hildreth, W., The timing of caldera collapse at Mount Katmai in response to magma withdrawal toward Novarupta, *Geophys. Res. Lett.*, *18*, 1541–1544, 1991.

Lu, Z., and J. Freymueller, Synthetic aperture radar interferometry coherence analysis over Katmai volcano group, Alaska, *J. Geophys. Res.*, *103*, 29,887–29,894, 1998.

Lu, Z., D. Mann, J. Freymueller, and D. Meyer, Synthetic aperture radar interferometry of Okmok volcano, Alaska: Radar observations, *J. Geophys. Res.*, *105*, 10,791–10,806, 2000a.

Lu, Z., C. Wicks, D. Dzurisin, W. Thatcher, J. Freymueller, S. McNutt, and D. Mann, Aseismic inflation of Westdahl volcano, Alaska, revealed by satellite radar interferometry, *Geophys. Res. Lett.*, *27*, 1567–1570, 2000b.

Lu, Z., C. Wicks, J. Power, and D. Dzurisin, Ground deformation associated with the March 1996 earthquake swarm at Akutan volcano, Alaska, revealed by satellite radar interferometry, *J. Geophys. Res.*, *105*, 21,483–21,496, 2000c.

Lu, Z., C. Wicks, D. Dzurisin, J. Power, S. Moran, and W. Thatcher, Magmatic inflation at a dormant stratovolcano: 1996–1898 activity at Mount Peulik volcano, Alaska, revealed by satellite radar interferometry, *J. Geophys. Res.*, *107*(B7), 2134, doi:10.1029/2001JB000471, 2002.

Massonnet, D., and K. Feigl, Radar interferometry and its application to changes in the Earth's surface, *Rev. Geophys.*, *36*, 441–500, 1998.

Massonnet, D., P. Briole, and A. Arnaud, Deflation of Mount Etna monitored by spaceborne radar interferometry, *Nature*, *375*, 567–570, 1995.

McCann, G. D., and C. H. Wilts, A mathematical analysis of the subsidence in the Long Beach-San Pedro Area, internal report, Calif. Inst. of Technol., Pasadena, Calif., Nov. 1951.

McConnell, V. R., J. E. Beget, A. L. Roach, K. W. Bean, and C. L. Nye, Geologic map of the Makushin volcanic field, Unalaska Island, Alaska, *Rep. Invest. 97-20*, 2 sheets, scale 1:63360, Alaska Div. of Geol. and Geophys. Surv., Fairbanks, 1997.

McGimsey, R. G., and C. A. Neal, 1995 volcanic activity in Alaska: Summary of events and responses to the Alaska Volcano Observatory, *U.S. Geol. Surv. Open File Rep., 96-738*, 1996.

Miller, T. P., R. G. McGimsey, D. H. Richter, J. R. Riehle, C. J. Nye, M. E. Yount, and J. A. Dumoulin, Catalog of the historically active volcanoes of Alaska, *U.S. Geol. Surv. Open File Rep.,98-582*, 1998.

Mogi, K., Relations between the eruptions of various volcanoes and the deformations of the ground surface around them, *Bull. Earthquake Res. Inst. Univ. Tokyo*, *36*, 99–134, 1958.

NASA, Landsat 7 Science Data Users Handbook, http://ltpwww.gsfc.nasa.gov/IAS/handbook/handbook_site_map.html, 1999.

Neal, C. A., M. P. Doukas, and R. G. McGimsey, 1994 volcanic activity in Alaska and Kamchatka: Summary of events and responses to the Alaska Volcano Observatory, *U.S. Geol. Surv. Open File Rep., 95-271*, 1995.

Neal, C. A., R. G. McGimsey, and M. P. Doukas, 1993 volcanic activity in Alaska: Summary of events and responses to the Alaska Volcano Observatory, *U.S. Geol. Surv. Open File Rep., 96-24*, 1996.

Newhall, C. G., and D. Dzurisin, Historical unrest at large calderas of the world, *U.S. Geol. Surv. Bull., 1855*, 1108 pp., 1988.

Nye, C. J., Makushin: Eastern Aleutian Islands, in *Volcanoes of North America*, edited by C. A. Wood and J. Kienle, pp. 41–43, Cambridge Univ. Press, New York, 1990.

Press, W., S. Teukolsky, W. Vetterling, and B. Flannery, *Numerical Recipes in C, the Art of Scientific Computing*, 994 pp., Cambridge Univ. Press, New York, 1992.

Roach, A. L., and V. S. McConnell, Historical evolution of the summit crater of Makushin Volcano, Unalaska Island, Alaska, *Eos Trans. AGU*, *77*(46), F771–F772, Fall Meet. Suppl., 1996.

Rosen, P. A., et al., Synthetic aperture radar interferometry, *Proc. IEEE*, *88*, 333–380, 2000.

Sabins, F. F., *Remote Sensing Principles and Interpretation*, 3rd ed., W. H. Freeman, New York, 1997.

Sigmundsson, F., P. Durand, and D. Massonnet, Opening of an eruptive fissure and seaward displacement at Piton de la Fournaise volcano measured by RADARSAT satellite radar interferometry, *Geophys. Res. Lett.*, *26*, 533–536, 1999.

Simkin, T., and L. Siebert, *Volcanoes of the World*, 2nd ed., 349 pp., Geosci. Press, Tucson, Ariz., 1994.

Smithsonian Institution, *Bulletin of Global Volcanism Network*, *20*(1), 1995.

Vadon, H., and F. Sigmundsson, Crustal deformation from 1992 to 1995 at the Mid-Atlantic Ridge, southwest Iceland, mapped by satellite radar interferometry, *Science*, *275*, 193–197, 1997.

Wegmuller, U., and C. Werner, Retrieval of vegetation parameters with SAR interferometry, *IEEE Trans. Geosci. Remote Sens.*, *35*, 18–24, 1997.

Wicks, C., W. Thatcher, and D. Dzurisin, Migration of fluids beneath Yellowstone Caldera inferred from satellite radar interferometry, *Science*, *282*, 458–462, 1998.

Wicks, C. W., D. Dzurisin, S. Ingebritsen, W. Thatcher, Z. Lu, and J. Iverson, Magmatic activity beneath the quiescent Three Sisters volcanic center, central Oregon Cascade Range, USA, *Geophys. Res. Lett.*, *29*(7), 1122, doi:10.1029/2001GL014205, 2002.

Williams, C. A., and G. Wadge, The effects of topography on magma chamber deformation models: Application to Mt. Etna and radar interferometry, *Geophys. Res. Lett.*, *25*, 1549–1552, 1998.

Zebker, H. A., and J. Villasenor, Decorrelation in interferometric radar echoes, *IEEE Trans. Geosci. Remote Sens.*, *30*, 950–959, 1992.

Zebker, H., F. Amelung, and S. Jonsson, Remote sensing of volcano surface and internal processing using radar interferometry, in *Remote Sensing of Active Volcanism*, *Geophys. Monogr Ser.*, vol. 116, edited by P. J. Mouginis-Mark, J. A. Crisp, and J. H. Fink, pp. 179–205, AGU, Washington, D. C., 2000.

D. Dzurisin, U.S. Geological Survey, David A. Johnston Cascades Volcano Observatory, 1300 S.E. Cardinal Court, Suite 100, Vancouver, WA 98683-9589, USA. (dzurisin@usgs.gov)

Z. Lu, U.S. Geological Survey, EROS Data Center, Raytheon ITSS, Sioux Falls, SD 57198, USA. (lu@usgs.gov)

V. S. McConnell, Oregon Department of Geology and Mineral Industries, 1510 Campbell St., Baker City, OR 97814, USA. (vdogami@OregonVOS.net)

J. A. Power, U.S. Geological Survey, Alaska Volcano Observatory, 4200 University Drive; Anchorage, AK 99508, USA. (jpower@usgs.gov)

C. Wicks Jr., U.S. Geological Survey, 345 Middlefield Rd., MS 977, Menlo Park, CA 94025-3591, USA. (cwicks@usgs.gov)